CORE
Metadata, citation and similar papers at core.ac.uk
Provided by Electronic Sumy State University Institutional Repository

PROCEEDINGS OF THE INTERNATIONAL CONFERENCE NANOMATERIALS: APPLICATIONS AND PROPERTIES
Vol. **1** No 4, 04PITSE09(4pp) (2012)

Advanced Ion and Plasma Sources for Materials Surface Engineering

A.F. Alexandrov, E.A. Kralkina, P.A. Nekludova, V.B. Pavlov, A.K. Petrov, K.V. Vavilin

Physical Faculty of MSU, 119991, GSP-2, Moscow, Vorobjevy Gory

(Received 20 June 2012; published online 24 August 2012)

The paper presents the results of the authors many year work in the field of ion&plasma sources development. The families of DC and RF ion and plasma sources are described. The results of ion&plasma sources utilization in materials surface modification technologies are discussed.

Keywords: Ion Source, Plasma Source, Surface Modification, Plasma, Ion Beam.

PACS number: 52.50.Dg.

1. INTRODUCTION

During last decades the trend became evident to utilize ion beam and plasma technologies in industrial applications [1]. The reason consists in wide possibilities and ecological compatibility of the ion beam and plasma processes. A lot of plasma sources models are known nowadays [1-13]. However the development of science and industrial technologies requires more flexible, more energy efficient, more perfect plasma sources.

The paper presents the results of the authors many year work in the field of ion&plasma sources development as well as the results of their utilization in materials surface modification technologies.

2. THE FAMILY OF DC IS

The distinguishing feature of the DC IS family (30, 50 and 100 mm in diameter) is the use of the glow discharge for electrons generation in the water cooled hollow cathode (cold cathode). The absence of filament or "hot-hollow" cathode provides long life time of the IS even in case of reactive gases utilization.

2.1 The Construction of DC IS

The scheme of the DC IS is shown on Fig. 1.

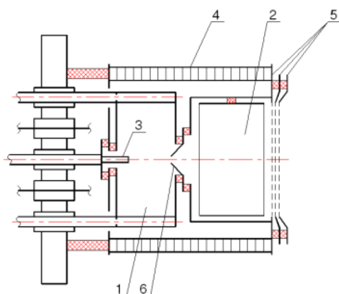

Fig. 1 – Construction of the cold cathode ion source. 1, 2 – cathode and anode chambers; 3 – gas distributor, 4 -magnetic system; 5 - ion optic system; 6 – cone orifice

Cold cathode ion source (see Fig. 1) consists of cylindrical water cooled cathode 1, cylindrical anode 2, gas distributor 3, magnetic system 4 providing magnetic field in the cathode and anode chambers and ion extraction system (IOS) 5. Between cathode and anode chambers a cone orifice 6 is executed. It connects cathode and anode blocks.

2.2 Characterization of DC IS

Experiments showed that plasma potential measured in the anode chamber was close to the anode one, electron energy distribution was highly enriched by the group of fast electrons. It should be also noted that spatial distribution of electrons is defined mainly by magnetic field configuration and doesn't depend on diameter of the orifice connecting cathodic and anode chambers if its diameter doesn't exceed 5mm.

Fig. 2 shows the extracted argon ion beam current i_b versus the discharge current i_d. One can see that ion beam current is proportional to the discharge one in the wide range of i_d.

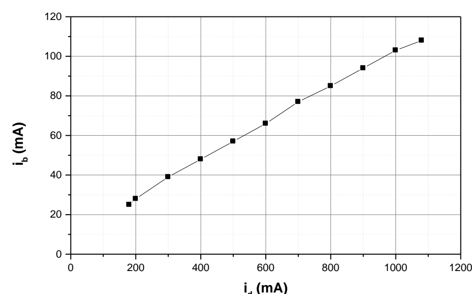

Fig. 2 – The extracted argon ion beam current versus the discharge current. Argon flow rate is equal to 2.5 cm³/min. Ion source diameter is 50 mm

DC IS (30, 50 and 100 mm in diameter) provide ion beam current density ranging from 0.5 to 4.5 mA/cm², ion energy can be varied within 200-1500 eV.

Fig. 3 represents radial dependence of the ion beam current density. The curve was obtained with flat electrodes of the IOS. The utilization of the profiled electrodes of the IOS leads to more homogeneous $i_b(r)$ distribution however the ion beam current density becomes lower.

3. DC RADICAL SOURCE

DC radical source (RS) is the modified DS IS. The construction of DC RS differs from the DC IS one by the absence of IOS. It is changed by the grounded perforated electrode. The presence of fast electrons in the discharge leads to the high dissociation rate of the working molecular gas and gives the opportunity to obtain a flow of plasma enriched by the products of

 © 2012 Sumy State University

molecules dissociation at the exit of DS RS. The dependence of nitrogen and oxygen dissociation degree on discharge current is shown on Fig. 4.

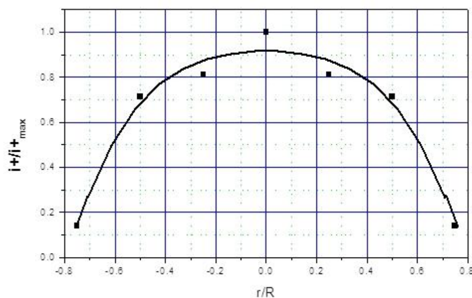

Fig.3. Radial dependence of the ion beam current density near the exit of the 50mm in Diameter DC IS.

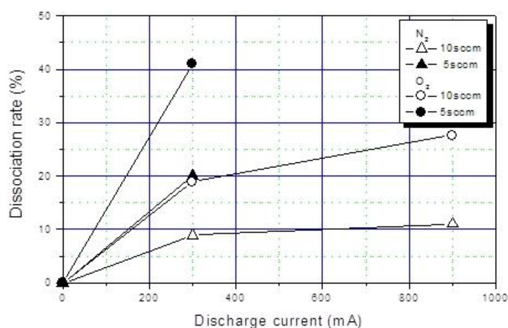

Fig. 4 – Dissociation rate versus discharge current.

4. RF GRIDDED ION SOURCE FAMILY

Since the last decade of the XX the systematic research of RF power absorption mechanism was conducted by the authors of the present paper [13]. The main attention was concentrated on revealing the conditions of efficient RF power input to plasma and high plasma density generation. It was shown that at pressure less than 10 mTorr the most efficient RF power absorption can be achieved under conditions of resonant helicons and oblique Langmuir waves excitation. That is the reason why inductive RF discharge located in an external magnetic field of certain vale, became a basic working process of the original family of RF gridded IS.

4.1 The construction of RF gridded IS

RF IS source consists of the dielectric gas-discharge chamber (GRC), magnetic and ion-optical systems. The magnetic system is based on electromagnets. The ion-optical system consists of three punched electrodes.

Cylindrical RF IS with diameter 100 and 200MM as well as linear RF IS with the IOS size 20 × 15cm are developed.

For ignitions and maintenance of the discharge the cooled spiral antenna located on a lateral or face external surface of GRC are used. The ends of the antenna are connected to the RF power supply through the matching system.

4.2 Characterization of RF gridded IS

Fig. 5 shows the dependences of ion beam current on the RF generator power. One can see that sources are efficient when using both inert, and chemically active gases.

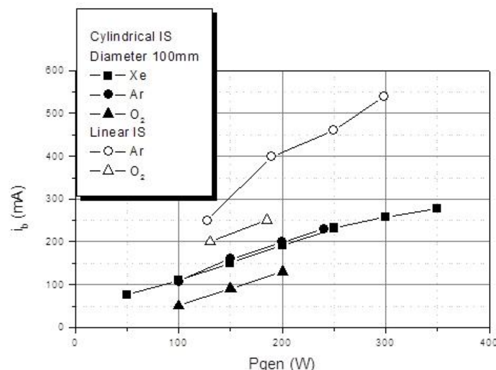

Fig. 5 – Ion beam current versus RF generator power.

Spatial distribution of ion beam current density is of great interest for industrial applications. One of the most important factors influencing a profile of an ion current density is the value of an external magnetic field (see Fig.6). Fig.7 represents radial distribution of an ion beam current density measured at different distances from the RF IS IOS. The magnetic field value corresponds to the best conditions of RF power absorption by plasma.

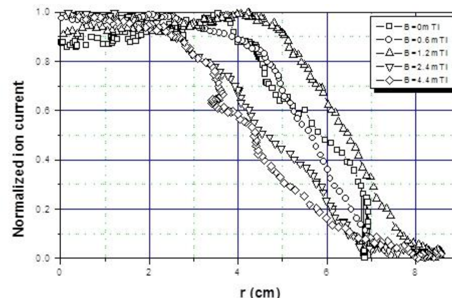

Fig. 6 – Radial dependencies of the normalized ion beam current density measured near IOS.

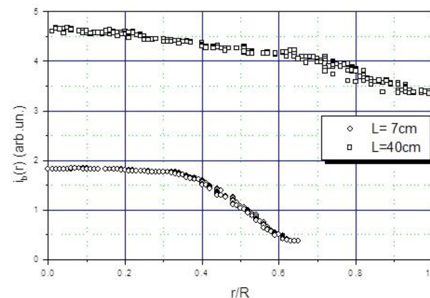

Fig. 7 – Radial dependencies of the ion beam current density measured at the different distances from IOS.

The ion beam energy can be changed from 50 to 1500 eV. Thus the IS provides possibilities for "soft" (at energy of ions about 50 eV), and "rigid" (at energy of ions of an order 1000 eV), impacts on samples. However the ion beam current density in the case of 50 eV ion energy is low.

5. RF GRIDLESS ION SOURCE

In order to provide soft treatment of samples by of relatively high current ion beam the RF gridless IS was developed. The working process of the IS is also based on the inductive RF discharge located in the external magnetic field which value corresponds to the resonant conditions of helicons and oblique Langmuir waves excitation.

5.1 The construction of RF gridless IS

The IS consists of cylindrical dielectric gas discharge chamber with diameter 5cm and length 15cm (see Fig. 8). The working gas is supplied to the upper end of the discharge chamber while the other one ends with a Laval nozzle. The GDC is located in the external magnetic field provided by the electromagnet. The spiral antenna is assembled on the lateral side of the IS. Antenna ends are connected to the RF power source through the matching system.

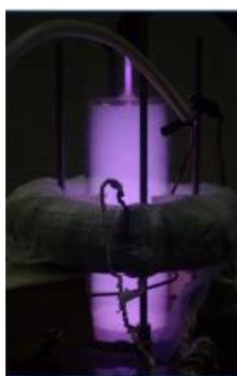

Fig. 8 – The laboratory model of RF gridless IS

5.2 Characterization of RF gridless IS

The ion energy distribution functions were measured in dependence on gas flow rate, power input and magnetic field value. Measurements revealed the existence of two groups of ions, i.e. slow (with energy about 30 eV) and fast ones (with energy 60-170 eV). The gas flow rate increase leads to the reduction of the high-energy ions number and enhancement of the slow ones quantity. Typical ion beam energy distribution function obtained at Ar flow rate 6cm^3/min is shown on Fig. 9.

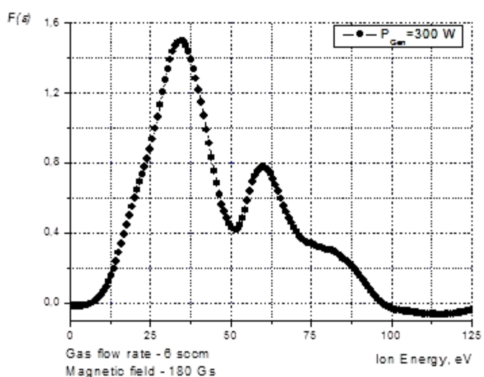

Fig. 9 – Typical ion beam energy distribution

6. THE PROLONGED PLASMA SOURCE WORKING AT ATMOSPHERIC PRESSURE

6.1 The construction of atmospheric plasma source

The prolonged plasma source [14-16] (see Fig. 10) includes ignition and main electrodes, RF power input unit, gas distributor providing air or working gas flow. The discharge is ignited between the main electrode and the sample, placed on the grounded plane. The advantages of RF plasma source are the possibility of thick dielectric substrates processing and low ozone generation rate.

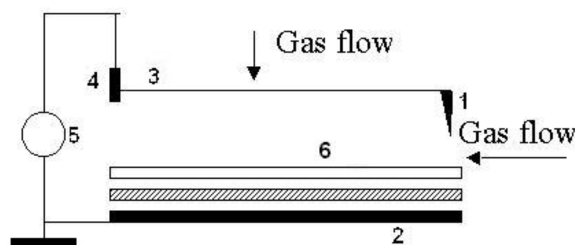

Fig. 10 – The scheme of the prolonged plasma source. 1 – ignition electrode, 2- grounded plate, 3 – main electrode, 4 – RF power input unit, 5 – RF power supply, 6 – sample

6.2 The properties of atmospheric plasma source

Fig. 11 demonstrates the distribution of nitrogen molecule and molecular ion radiation intensity in the gap between the main electrode and the grounded plane. If discharge occupies the whole gap the maxima of radiation intensity can be observed near the electrodes. The appearance of the radiation maxima can be attributed to a formation of the spatial charge sheaths. A potential drop that accelerates ions towards electrodes is known to appear along the sheath. The sheath presence near the place where the samples are located indicates a significant role of the accelerated ions in the change of properties of processed materials as in the case of low pressure plasma.

Measurement of the radiation intensity in various points along the main electrode showed high uniformity of the discharge.

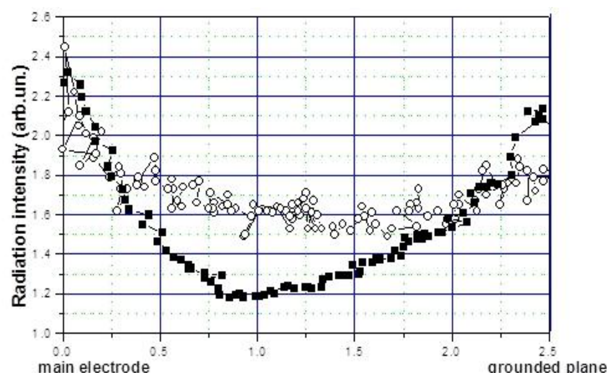

Fig. 11 – Nitrogen molecule (open circles) and molecular ion (filled squares) radiation intensity distribution in an interval between the main electrode and the grounded plane

7. APPROBATION OF ION&PLASMA SOURCE IN SURFACE MODIFICATION TECHNOLOGIES

The developed ion&plasma sources were approved in modern surface modification technologies. The results of PTFE surface modification are shown on Fig. 12. The irradiation of PTFE samples leads to significant improvement of its adhesion. The presence of oxygen especially enriched by radicals during the irradiation of samples by argon is accompanied by further increase of the adhesive force. Irradiation of PTFE samples only by a flow of the oxygen enriched by radicals, leads to some improvement of adhesion but the result is much worse than in case of ion irradiation.

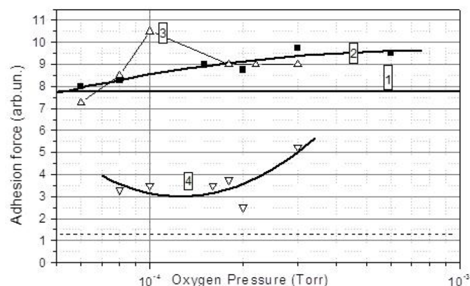

Fig. 12 – The PTFE adhesion force versus oxygen pressure. Dashed line corresponds to adhesion force of the untreated PTFE. 1,2,3,4 correspond to the irradiation of PTFE only by Ar ions, by Ar ions in the presence of oxygen, by Ar ions in the presence of oxygen enriched by radicals, only by oxygen enriched by radicals

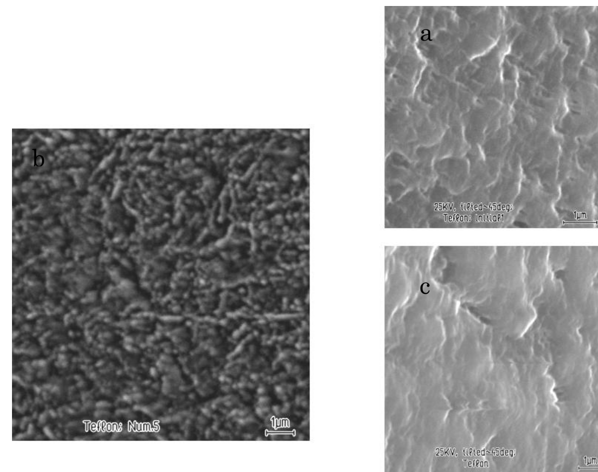

Fig. 13 – SEM pictures of PTFE surface: a) untreated PTFE, b) after ion beam irradiation, c) after treatment in atmospheric discharge

From all variety of the physical and chemical processes occurring on a PTFE surface [17] we will allocate two: the change of chemical properties of materials surface and change of the morphology of a surface. Experiments showed (see Fig.13) that irradiation of PTFE by the ion beam results in essential change of morphology of a surface, while the presence of chemically active particles, especially radicals, leads to the change of a chemical composition of a surface [18]. The treatment of PTFE by atmospheric discharge leads to smoothing and change in the chemical composition of its surface.

REFERENCES

1. *Handbook of plasma processing technology: fundamentals, etching,deposition, and surface interactions. (*Edited by S.M. Rossnagel, J.J. Cuomo and W.D. Westwood), (Noyes Publications, 1990, 523p).
2. H.R. Kaufman and R.S. Robinson. *Operation of broad-beam sources*. (Commonwealth Scientific Corporation, Alexandria, Virginia, 1987) 201p.
3. *Handbook of plasma processing technology: fundamentals, etching, deposition, and surface interactions.* (Edited by S.M. Rossnagel, J.J. Cuomo and W.D. Westwood), (Noyes Publications, 1990) 523.
4. H.R. Kaufman and R.S. Robinson. *AIAA J.* **20**, 745 (1982).
5. *Plasma accelerators and ion injectors* (Ed. by N.P. Kozlov and Alexander Morozov), (Nauka, Moscow, 1984), 272.
6. S. Kadoma, S. Suzuki. *Patent abstract of Japan 57011448 A*. Jan. 21, (1982).
7. N. Gavrilov. *Plasma emitted of ions.* RU 2134921 C1, Nov.20, (1997).
8. N. Gavrilin, D. Emlin, S. Nikulin. *Tech. Phys. Lett.* **25** No12, 83 (1995).
9. http://www.orc.ru/~platar/ PLATAR Ltd., 24.05.2000.
10. G.E. Bugrov, S.K. Kondranin, E.A. Kralkina, V.B. Pavlov, K.V. Vavilin, Heon-Ju Lee. *J. of Korean Vacuum Science & Technology*, **5**, 19 – 24 (2001).
11. G.E. Bugrov, S.G. Kondranin, E.A. Kralkina, V.B. Pavlov, D.V. Savinov, K.V. Vavilin, Heon-Ju Lee. *Curr. Appl. Phys.* **3**, 485 (2003).
12. K.V. Vavilin, E.A. Kral'kina, V.B. Paul, K. Ko, C.S. Lee. patent RU 2371803, 2008.
13. E.A. Kral'kina, *Phys.-Usp.* **51**, 493 (2008).
14. A.F. Alexandrov, G.E. Bougrov, S.K. Kondranin, E.A. Kralkina, V.B. Pavlov, A.A. Rukhadze, V.Yu. Sergeenko, I.B. Timofeev, K.V. Vavilin. *Proceedings of XXV International Conference on Phenomena in Ionized Gases,* 17-22 July 2001 Nagoya, Japan vol. 1, 35 – 36.
15. A.F. Alexandrov, E.A. Kralkina, V.B. Pavlov, V.P. Savinov, V.Yu. Sergeenko, I.B. Timofeev, G.E. Bugrov, K.V. Vavilin, V.Yu. Plaksin, Young Son Mok and Heon-Ju Lee. *J. Ceram. Proces. Res.* **8** No1, 64 (2007).
16. A.F. Alexandrov, G.E. Knolls, K.V. Vavilin, S.G. Kondranin, E.A. Kral'kina, V.J. Plaksin, V.J. Sergienko, I.B. Timofeev, B. Timofeev, patent RU 2196394.
17. *Plasma Surface Modification of Polymers: Relevance to Adhesion.* (Edited by M. Strobel, C.S. Lyons and K.L. Mittal), (Utrecht, The Netherlands, 1994), 290p.
18. S-K. Koh et al. *US patent* 5,783, 641, 1998; *US patent* 5,965,629, 1999; *US patent* 6,300,641B1, 2001.